Evaluation of Vertical Integrated Nanogenerator Performances in Flexion

2013 J. Phys.: Conf. Ser. 476 012006

(http://iopscience.iop.org/1742-6596/476/1/012006)

Evaluation of Vertical Integrated Nanogenerator Performances in Flexion

R Tao, R Hinchet, G Ardila and M Mouis

IMEP-LAHC, Grenoble-INP, Univ. J. Fourier, Univ. Savoie, CNRS , 3 Parvis L. Néel BP 257, 38016, Grenoble, France

E-mail: taoran07@gmail.com

Abstract. Piezoelectric nanowires have attracted great interest as new building blocks of mechanical energy harvesting systems. This paper presents the design improvements of mechanical energy harvesters integrating vertical ZnO piezoelectric nanowires onto a Silicon or plastic membrane. We have calculated the energy generation and conversion performance of ZnO nanowires based vertical integrated nanogenerators in flexion mode. We show that in flexion mode ZnO nanowires are superior to bulk ZnO layer. Both mechanical and electrical effects of matrix materials on the potential generation and energy conversion are discussed, in the aim of guiding further improvement of nanogenerator performance.

1. Introduction

Recently, piezoelectric nanowires (NWs) have attracted great interest as the fundamental building blocks for future electronic autonomous devices. Their unique electrical and mechanical properties can be exploited advantageously for applications such as sensors [1], piezoelectric diodes [2] and energy harvesting devices [3]. Among the latter, nanogenerators (NGs) have received much attention, where piezoelectricity is employed to convert mechanical energy to electrical energy for the operation of low-power electronics [4]. Given that the size-induced enhancement of electromechanical properties has been primarily reported for piezoelectric NWs [5], the development of new experimental, computational, and theoretical approaches is required to meet challenges at nanoscale. In this work, finite element method (FEM) simulations are used to calculate the energy generation and conversion performance of ZnO NWs based energy harvesters. The design of the devices is based on the Vertically Integrated NanoGenerator (VING) as proposed in [6].

2. Nanogenerator structure

The energy harvesting device (Figure 1) consists of a VING structure sandwiched between two aluminium electrodes on a substrate. The 1cm × 1cm substrate is made of silicon or plastic membrane: the former is compatible with current electric circuits and devices, while the latter is more flexible and adaptable to future independent self-powered nanosystems. As a continuation of previous work [7], Si membrane was used to calculate the strain distribution under given pressure. The functional core structure of the NG is the piezoelectric NWs integrated into a thin insulating PMMA layer. The NWs grow along their c-axis on a thin ZnO seed layer deposited using spattering. Si_3N_4 insulating layers with no internal strain avoid the short circuit and increase NG robustness. We have previously evaluated NGs under compression [7]. Here we extend the study to a flexion mode using a thin

membrane as a mechanical transducer. The hydrostatic pressure generates a force bending the membrane, compressing the NW from the sidewalls.

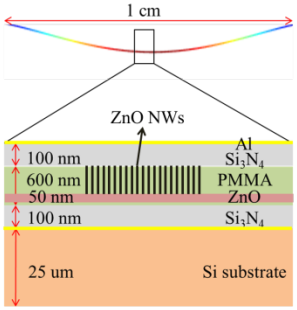

Figure 1. Cross-section view of the device with a zoom where the VING is located.

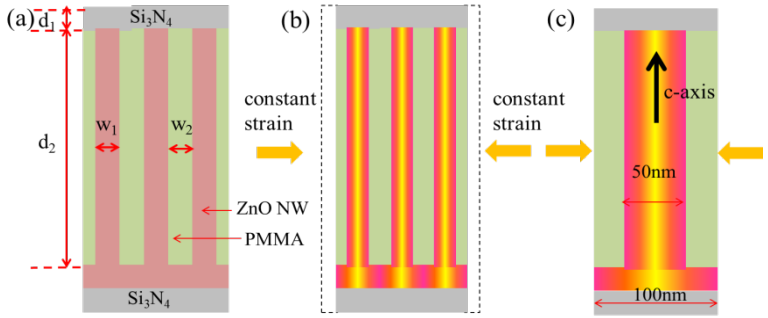

Figure 2. Schematic of nanogenerator cells structure. The radius of the NW is 25 nm and the width of the cell is 100 nm. When the membrane is bent, the single nanogenerator cell is compressed laterally.

3. Nanogenerator operation and modelling assumptions

Under strain, the NW active layer of the VING structure generates a potential difference which can be used to power an external circuit by means of a capacitive displacement current.

The hypothesis of an applied hydrostatic pressure is applied over the membrane structure (Figure 1). The main issue compared to previews studies [7] is how the constraint is transferred to the NW. For this reason, although the active part of the device is made of millions of NWs integrated into a polymer matrix, in this study only a single core cell of the device was considered (Figure 2c) with appropriate boundary conditions for fast and reliable FEM modeling.

When the device membrane is under flexion, the NG core cell is compressed laterally and extended along the c-axis (Figure 2). In the core cell, the energy conversion mechanism has been divided into 3 steps [7]: mechanical energy transfer, mechanical to electrical energy conversion and, finally, electrical energy transfer to the output circuit. In the first step, the total input mechanical energy ξ is considered to be composed of two parts. One (ξ_1) is the energy stored in the Si_3N_4 layers, and the other (ξ_2) is the energy stored in the NW/PMMA compound. The energy that reaches the core NW is used in the piezoelectric transfer process (ξ_3). Thus, the mechanical energy transfer efficiency is expressed as $\eta_m=\xi_3/(\xi_1+\xi_2)$, where ξ_1 is supposed to be a constant. Thus the major influencing factor is the ratio of ξ_3 and ξ_2, whose reciprocal increases with $(w_2E_{NW})/(w_1E_{PMMA})$ where w_1 and w_2 are geometrical parameters (see Figure 2) and E is the Young Modulus. The energy conversion efficiency η_p of the second step depends on the NW's electromechanical properties and is proportional to the square of piezoelectric strain constant e_{33}^2 [7]. The third step brings dielectric losses to our device with the efficiency (η_p) defined as $1/(1+d_1\varepsilon_{2eq}/d_2\varepsilon_1)$, where d is a geometrical parameter (see Figure 2), ε_{2eq} and ε_1 are the relative permittivity of the NW/matrix compound and the Si_3N_4 layer respectively. Finally the total conversion efficiency is the product of the three individual step efficiencies.

4. Simulation

FEM simulations of the device were performed. The coupling between the mechanical, electrical and piezoelectric equations was considered for a core NG cell. The input impact described by the strain in the cell was calculated from a 2D model of the membrane. Because the NW layer was far from neutral plane, the hydrostatic pressure generated constant strain at sidewalls of each cell along c-axis. We calculated that the NW/PMMA layer had a vertically homogeneous strain of -9.36×10^{-4} (within linear deformation) when the device is bent by a hydrostatic pressure of 1.8 kPa, which is the limit of the linear deformation regime. The cell size was 100nm × 100nm × 850nm, with NW radius r=25nm and length L=600nm. Young's modulus, Poisson's ratio (υ) and relative permittivity of the matrix material were varied around parameters of PMMA in order to investigate optimization trends. Several real

insulating compounds were used as the matrix material. Their functions on potential generation and energy conversion were compared with each other, as well as with a ZnO layer (the thickness is 118 nm) which has the same volume as ZnO NW.

Analysis is focused on the displacement, the strain tensor S_{xx} and the electric potential distributions. The hardness of the matrix material results in two different types of distribution of the displacement and the strain. When a soft matrix material (PMMA) was used, the matrix was more compressed than the NW as indicated by the displacement distribution (Figure 3a). The strain tensor S_{xx} distribution (Figure 3b) shows that strain was concentrated in the matrix material instead of the NW. The opposite resulted when a hard matrix (Al_2O_3) was used (Figure 3c) and strain is concentrated in the NW (Figure 3d). This is consistent with the mechanical energy transfer efficiency (η_m) defined in section 3. As the Young's modulus of the matrix material increases, the efficiency increases. More mechanical energy is transferred into the core NW, influencing the final potential and energy generation.

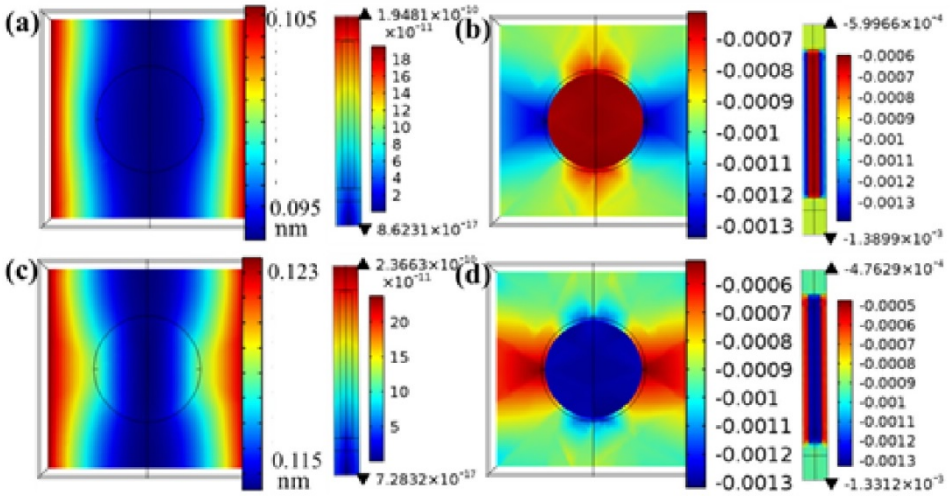

Figure 3. Topview and sideview mapping of (a) displacement and (b) strain when PMMA is used; (c) displacement and (d) strain when Al_2O_3 is used.

Several insulating matrix materials were considered to improve the NG performances. In the simulations, the total volume of ZnO was kept constant. The potential (Figure 4) was calculated along the central axis of the NG cell. From simulations, the potential generation ability of bulk ZnO (yellow line) is weaker than that of NW based NG cells. Zones (1) and (4) correspond to the Si_3N_4 insulating layers, where dielectric losses are unavoidable. Zone (2) corresponds to the thin seed ZnO layer, while zone (3) is corresponding to the NW layer. Globally, the NG cell with harder matrix materials (Al_2O_3, Si_3N_4) generated higher potential.

To clarify the energy transfer process, Young's modulus, Poisson's ratio and relative permittivity of matrix materials were varied independently. The former two parameters mainly influence the mechanical energy transfer and slightly affect the piezoelectric energy transfer. The relative permittivity affects the electrical energy transfer to the output circuit. Mechanical and electrical parameters of real matrix materials are listed in Table 1. First, the effects of Young's modulus and Poisson's ratio on the potential generation were compared (Figure 5). The curves were plotted against one parameter while the two others were kept equal to that of PMMA. As the value of Young's modulus spans from 3GPa (PMMA) to 400GPa (Al_2O_3), the potential increases from 0.8V to 4.4V. In contrast, varying from 0.17 to 0.40, the change of Poisson's ratio only brings a potential difference of 1V. The relationship between the relative permittivity and the electric potential is more complex. In fact, the relative permittivity of the matrix material is not the direct factor that influences the electrical energy transfer process. Efficiency η_e decreases with increasing ε_{eq} of the matrix/NW compound. Here

ε_{eq} is not a linear combination of the permittivity of the NW and the matrix. As a result, the potential curve reaches a maximum value when the permittivity is close to 2.5 (Figure 6). Considering that the relative permittivity of real matrix materials varies from 2.09 (SiO_2) to 9.7 (Si_3N_4), the potential variation is less than 0.5V. In the simulation, the effect of Young's modulus is more significant than the effects of Poisson's ratio and relative permittivity.

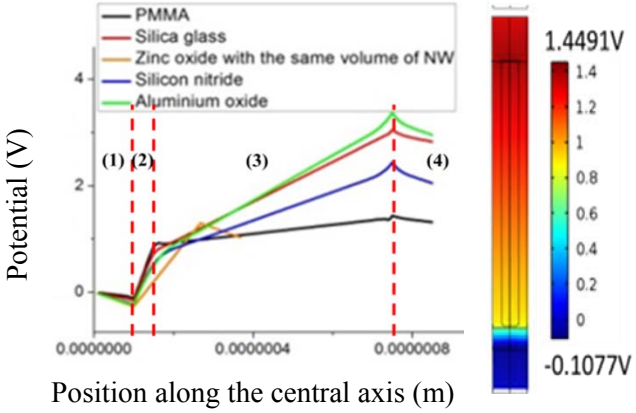

Figure 4. Potential distribution with different matrix materials along central axis (left). Sideview of potential distribution with PMMA matrix (right).

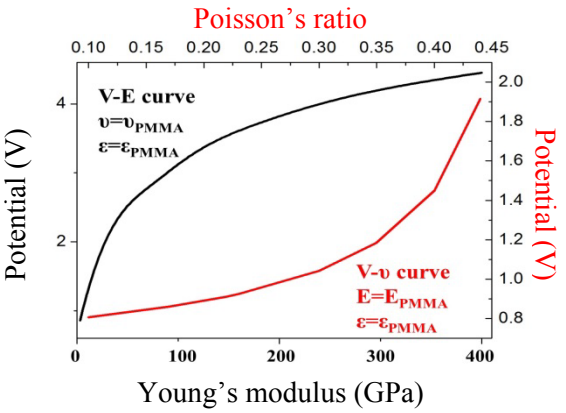

Figure 5. The potential changing trend with the increasing Young's modulus and Poisson's ratio of matrix materials.

Table 1. Mechanical and electrical parameters of different matrix materials.

	PMMA	SiO_2	ZnO	Si_3N_4	Al_2O_3
Young's modulus (GPa)	3	73.1	111	250	400
Poisson's ratio	0.40	0.17	0.35	0.23	0.22
Relative permittivity	3.0	2.09	8.9	9.7	5.7

The relationship between Young's modulus and the energy transfer process is discussed in Figure 7, 8 and 9. The solid line represents the simulation results of a material with fixed Poisson ratio (0.4) and relative permittivity (3.0) changing with increasing Young's Modulus, while the symbols represent simulation results for real matrix materials. At constant input strain, the strain energy is proportional to the equivalent Young's modulus of the matrix/NW compound, which means that more strain energy is needed to compress the NG cell with harder matrix material. With constant Poisson's ratio and relative permittivity, the total electric energy mainly benefits from the high mechanical energy transfer efficiency at high E. For hard materials, large relative permittivity reduces the electrical energy transfer to the output circuit. For PMMA, the low relative permittivity decreased the dielectric losses. The total energy conversion efficiency η is calculated by:

$$\eta = \frac{total\ electric\ energy}{total\ strain\ energy} = \eta_m \times \eta_p \times \eta_e \quad (1)$$

Within the different materials investigated, SiO_2 achieved the highest conversion efficiency with low relative permittivity and medium hardness.

The design has to be a compromise between mechanical energy transfer and electrical energy transfer. Low mechanical energy transfer obtained with soft materials can be translated into a low sensitivity of the device to external forces. On the other hand, low electrical energy transfer obtained with hard material (they usually have high relative permittivity) can increase the dielectric losses.

5. Conclusion

In this article, we have evaluated a VING structure working in flexion mode for the first time. The effect of matrix materials on NG cells was analyzed using FEM simulations, in order to improve the

device performance. Comparing with PMMA, a NG cell using an aluminum oxide matrix improves the potential by two times and the electric energy by six times which is essential for energy harvesters. On the other hand, silica glass will increase the energy conversion efficiency and could be better used in sensors applications.

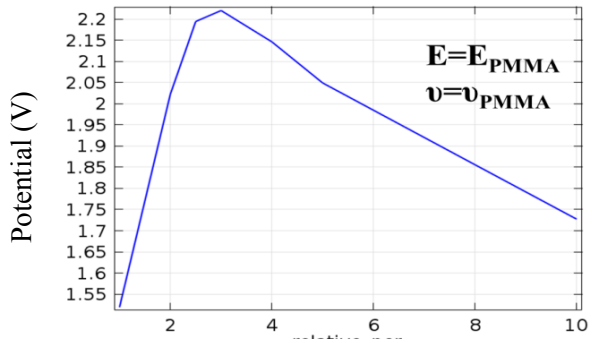

Figure 6. Potential changing with the increasing relative permittivity of matrix materials

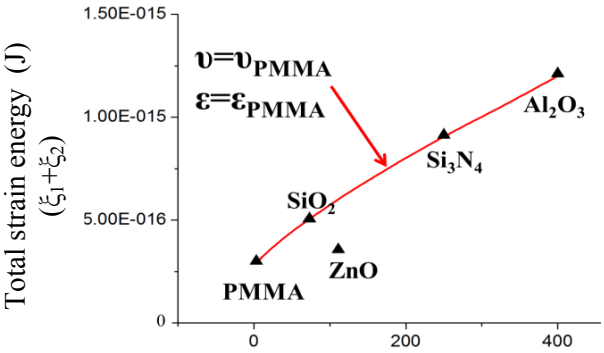

Figure 7. Total strain energy changing with the Young's modulus of matrix materials (per cell and per mechanical stimulus).

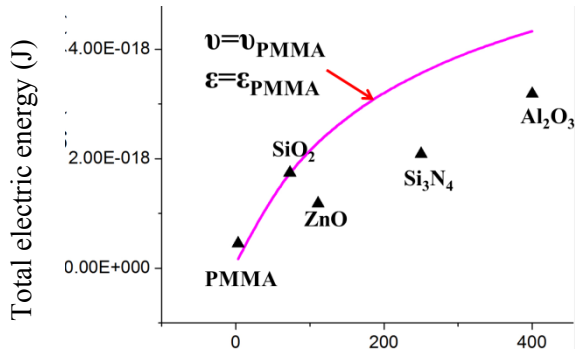

Figure 8. Total electric energy changing with the Young's modulus of matrix materials (per cell and per mechanical stimulus).

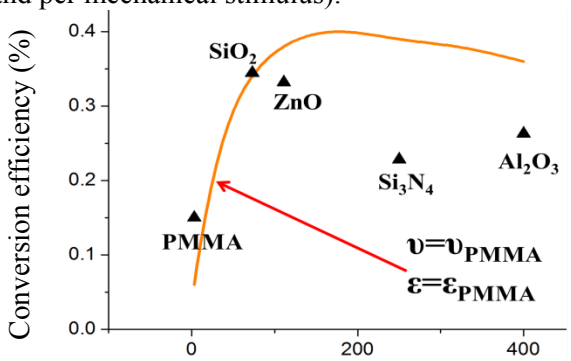

Figure 9. Energy conversion efficiency changing with the Young's modulus of matrix materials.

6. Acknowledgement

This work has been supported by CNRS INSIS Institute within the framework of Exploratory Projects on energy.

References

[1] Zhou J, Fei P, Gao Y F, Liu J, Bao G and Wang Z L 2008 *Nano Lett.* **8** 2725
[2] He J H, Hsin C L, Liu J, Chen L J and Wang Z L 2007 *Adv. Mater.* **19** 781
[3] Wang Z L and Song J 2006 *Science* **312** 242
[4] Hu Y, Zhang Y, Xu C, Zhu G and Wang Z L 2010 *Nano Lett.* **10** 5025
[5] Hinchet R, Ferreira J, Keraudy J, Ardila1 G, Pauliac-Vaujour E, Mouis M and Montès L 2012 Scaling rules of piezoelectric nanowires in view of sensor and energy harvester integration *IEDM, 2012 IEEE Int. (San Francisco, CA, 10-13 December 2012)* p 6.2.1 - 6.2.4
[6] Xu S, Qin Y, Xu C, Wei Y, Yang R and Wang Z L 2010 *nature nanotech.* **5** 367
[7] Hinchet R, Lee S, Ardila G, Montes L, Mouis M and Wang Z L Design and guideline rules for the performance improvement of vertically integrated nanogenerator *PowerMEMS 2012 (Atlanta, USA, 2-5 December 2012)*